Broadband and High-Filtering-Efficiency Band-Rejection Filters Fabricated Using Femtosecond Laser Line-by-Line Technology

Yu Fan , Weijia Bao , Cailing Fu, Changrui Liao, and Yiping Wang

Abstract—We have proposed and experimentally demonstrated a broadband-adjustable band-rejection filter based on a chirped and tilted fiber Bragg grating (CTFBG). The CTFBG is fabricated using femtosecond laser line-by-line technology. By precisely controlling the tilt angle, chirp rate, and pitch of the CTFBG, the filter's parameters such as wavelength, bandwidth, and efficiency can be flexibly customized. Through increasing the length of CTFBG, the large bandwidth and ultra-high filtering efficiency at the specific wavelength can be realized simultaneously. The proposed filter exhibits adjustable bandwidth ranging from 51 nm to 112 nm, low insertion loss (<1 dB), high filtering efficiency (up to >99.99%), and negligible back-reflection (<-30 dB). Moreover, the filters are insensitive to temperature, axial strain, and bending variations, which demonstrates their excellent spectral stability and robustness against disturbances.

Index Terms—Band-rejection filter, chirped and tilted fiber bragg grating, femtosecond laser, line-by-line.

I. INTRODUCTION

IBER Bragg grating (FBG) has been widely used in communication, sensing, laser technology and other applications as a band-rejection filter in recent years. In previously reported works, the commonly used fiber band-rejection filters were mainly focused on uniform FBG (UFBG) [1], [2], chirped FBG (CFBG) [3], [4], tilted FBG (TFBG) [5], [6] and long-period fiber grating (LPFG) [7], [8]. However, the UFBG and CFBG are difficult to match the filtering application

Received 9 March 2025; revised 22 April 2025 and 12 May 2025; accepted 4 June 2025. Date of publication 9 June 2025; date of current version 16 August 2025. This work was supported in part by the National Key Research and Development Program of China under Grant 2023YFB3209500, in part by the National Natural Science Foundation of China under Grant U22A2088, in part by Shenzhen Science and Technology Program under Grant JCYJ20241202124226032, in part by the Shenzhen Key Laboratory of Ultrafast Laser Micro/Nano Manufacturing under Grant ZDSYS20220606100405013, and in part by the Scientific Foundation for Youth Scholars of Shenzhen University under Grant 806-0000340610. (Corresponding author: Weijia Bao.)

The authors are with the Shenzhen Key Laboratory of Photonic Devices and Sensing Systems for Internet of Things, Guangdong and Hong Kong Joint Research Centre for Optical Fibre Sensors, State Key Laboratory of Radio Frequency Heterogeneous Integration, Shenzhen University, Shenzhen 518060, China, and also with the Shenzhen Key Laboratory of Ultrafast Laser Micro/Nano Manufacturing, Key Laboratory of Optoelectronic Devices and Systems of Ministry of Education/Guangdong Province, College of Physics and Optoelectronic Engineering, Shenzhen University, Shenzhen 518060, China (e-mail: 2350453012@email.szu.edu.cn; wjbao@szu.edu.cn; fucailing@szu.edu.cn; cliao@szu.edu.cn; ypwang@szu.edu.cn).

Color versions of one or more figures in this article are available at https://doi.org/10.1109/JLT.2025.3577737.

Digital Object Identifier 10.1109/JLT.2025.3577737

to their limited filtering bandwidth [1], [4]. And, although TFBG and LPFG have broadband filtering capabilities, the TFBG is limited by its non-smooth comb-like spectrum, which leads to a low filtering slope-efficiency [6], and the LPFG is limited by its over-sensitivity to the external environment, resulting in its unstable filtering characteristics [7]. Therefore, the above devices are difficult to achieve high-quality band-rejection filtering applications. Chirped and tilted fiber Bragg grating (CTFBG) could offer another interesting choice for such applications. The CTFBGs have the advantages of large filtering bandwidth (up to more than 100 nm), high filtering slope efficiency and exceptional broadband tunability, which makes them increasingly used in high-quality band-rejection filtering, edge filtering, and gain equalizers [9], [10], [11]. At present, the mainly used fabrication technology of CTFBG is ultraviolet (UV) laser phase mask technology [12], [13], which has the advantages of mature fabrication process and relatively low cost. However, hydrogen loading, which is a time-consuming and high-risk procedure of this technology, is an inevitable process before the fabrication of FBG [14], [15]. In addition, due to the opacity of the fiber coating to the UV laser, the coating must be stripped before fabrication, resulting in a decrease in the mechanical strength and toughness of the fiber device, which is not conducive to the practical application in a variety of complex environment filtering applications [12], [13], [14], [15], [16]. Moreover, the use of a phase mask makes most of the parameters of the CTFBG usually fixed and cannot be changed [10], [13]. Femtosecond laser direct writing technology is regarded as a promising alternative to the UV laser phase mask technology. It is such a flexible and adjustable technology, which can directly fabricate fiber devices through the coating. In recent years, it has been widely used in the fabrication of FBG devices [17], [18]. Femtosecond laser direct writing technology mainly includes three methods, i.e., pointby-point [19], line-by-line (LBL) [20] and plane-by-plane [21]. Duan et al. demonstrated the plane-by-plane inscription of CTF-BGs using a femtosecond laser slit-shaping technology, but the non-uniform modulation resulted in relatively high insertion loss in the fabricated devices [22]. Among other methods, the LBL technology is considered a promising method for fabricating high-quality CTFBGs due to its precision and flexibility in tilt angle control, as well as its ability to maintain low insertion loss.

requirements of large bandwidth (hundred-nanometer level) due

In this letter, high-filtering-efficiency and broadbandadjustable band-rejection filters based on CTFBG were directly

0733-8724 © 2025 IEEE. All rights reserved, including rights for text and data mining, and training of artificial intelligence and similar technologies. Personal use is permitted, but republication/redistribution requires IEEE permission. See https://www.ieee.org/publications/rights/index.html for more information.

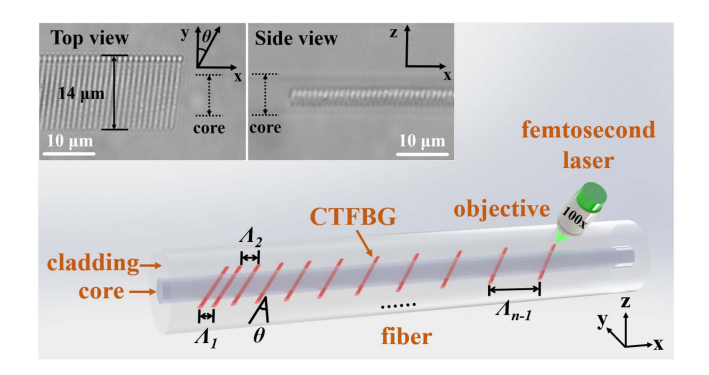


Fig. 1. Schematic diagram for fabricating CTFBG in SMF using femtosecond laser LBL technology. Inset: Top-view and side-view microscope images of a fabricated CTFBG in SMF.

fabricated using femtosecond laser LBL technology without any additional processing. The obtained CTFBGs exhibit low insertion loss (<1 dB), large and adjustable filtering bandwidth (51 nm–112 nm), high filtering efficiency (up to >99.99%) and a negligible back-reflection (<-30 dB). We experimentally verified that the fabrication parameters of CTFBGs such as pitch, tilt angle and chirp rate could be flexibly controlled based on LBL technology, so as to achieve the customization of spectral parameters such as wavelength, bandwidth, and filtering efficiency. Moreover, the experimental results show that this filter is insensitive to temperature, axial strain and bending. The CTFBGs fabricated by LBL technology show significant improvements in spectral tailoring and coating maintaining, making it a great candidate for high-quality band-rejection filtering, edge filters and gain equalizers.

II. EXPERIMENTAL SETUP AND PRINCIPLE

As shown in Fig. 1, the CTFBGs were fabricated by using a femtosecond laser (Pharos, Light-Conversion) with a pulse duration of 290 fs, a central wavelength of 514 nm, and a repetition rate of 200 kHz in a single-mode fiber (SMF, YOFC, G652D) with a core diameter of 9 μ m through a 100x oil-immersion objective (NA = 1.25). The SMF was fixed on an assembled 3D high-precision air-bearing translation stage (Aerotech ABL1500-100, ABL1500-100, and ANT130V-5) which can move the fiber towards x, y and z-axis. Here, by precisely controlling the 3D translation stage and femtosecond laser through programming, the LBL technology was realized to fabricate CTFBGs. The process of fabricating a CTFBG is as follows: First, the femtosecond laser is focused 2.5 μ m outside the core boundary and inscribes a tilted line with a tilt angle of θ along the positive directions of the x-axis and y-axis, where the line has a component of 14 μ m in the y-axis direction. Subsequently, the translation stage moves back to the origin and then shifts a distance of Λ_1 along the x-axis to inscribe the next line with the same parameters. After that, the translation stage moves back again and shifts a distance of Λ_2 along the x-axis to inscribe the following line. By repeating the above-mentioned process, a CTFBG composed of n modulation lines could be finally obtained, where the intervals between each line, $\Lambda_1, \Lambda_2, \ldots$

 $\Lambda_{\text{n-1}}$, are increased linearly. The grating parameters, including pitch of Λ , tilt angle of θ , chirp rate of δ , track length and total length were all precisely controlled via 3D translation stage. Moreover, by further controlling the scanning velocity and laser pulse energy, a customized CTFBG spectrum could be realized.

The linearly changed pitch Λ_c of CTFBG at position z could be given by:

$$\Lambda_c(z) = \frac{\Lambda_m}{\left(1 - \delta \cdot \frac{z}{L}\right)\cos\theta} \left(-\frac{L}{2} \le z \le \frac{L}{2}\right) \tag{1}$$

where the $\Lambda_{\rm m}$, δ and L are the middle pitch, chirp rate and total length of CTFBG, the tilt angle θ is the angle between the modulation line and the radial direction of fiber. For the FBG, the central reflection wavelength of the core mode $\lambda_{\rm core}$ and the nth order cladding mode $\lambda_{\rm clad}$, n at the position z could be given by:

$$\lambda_{core}\left(z\right) = 2n_{core}\Lambda\left(z\right) \tag{2}$$

$$\lambda_{clad, n}(z) = (n_{core} + n_{clad, n}) \Lambda(z)$$
 (3)

where the $n_{\rm core}$ and $n_{\rm clad,\ n}$ represent the effective refractive index of the core mode and the n^{th} order cladding mode, respectively.

Therefore, the reflection bandwidth of the core mode and the nth order cladding mode after the expansion of the chirp effect could be given by:

$$\Delta \lambda_{core} \approx 2n_{core} \left(\Lambda_{\text{max}} - \Lambda_{\text{min}} \right)$$
 (4)

$$\Delta \lambda_{clad, n} \approx (n_{core} + n_{clad, n}) (\Lambda_{max} - \Lambda_{min})$$
 (5)

where the $\Lambda_{\rm max}$ and $\Lambda_{\rm min}$ correspond to the longest and shortest pitch of the grating. Based on (1), (4) and (5), it could be known that the reflection bandwidth of the core mode and the cladding mode depend on the pitch Λ , chirp rate δ , tilt angle θ and total length L. In addition, the tilt angle θ further determines the overall envelope of the cladding mode transmission spectrum, because the coupling efficiency between the core mode and each cladding mode is related to it [6]. These will be reflected in the subsequent discussion. Moreover, existing simulation results on CTFBGs [12], [23], [24], [25] provide additional support for the analysis presented below.

III. EXPERIMENTAL RESULTS AND DISCUSSION

As shown in Fig. 2(a), it can be observed that the CFBG ($\delta=30$ nm/cm, $\theta=0$) exhibits a narrow reflection bandwidth of 15 nm. In contrast, the TFBG ($\delta=0$, $\theta=15^{\circ}$) has a broadband, comb-like transmission spectrum with a wide bandwidth of 70 nm, characterized by numerous narrow-band discrete resonances. Meanwhile, the CTFBG ($\delta=30$ nm/cm, $\theta=15^{\circ}$) presents a smooth and continuous transmission spectral envelope with a wide bandwidth of 75 nm, which is attributed to the broadening and overlap of the discrete narrow-band resonances. Here, CFBG, TFBG, and CTFBG were all fabricated by femtosecond laser LBL technology with the same scanning velocity (0.3 mm/s), pulse energy (20 nJ) and total length (5 mm). Fig. 2(b)–(d) show the microscope images of these grating structures, respectively.

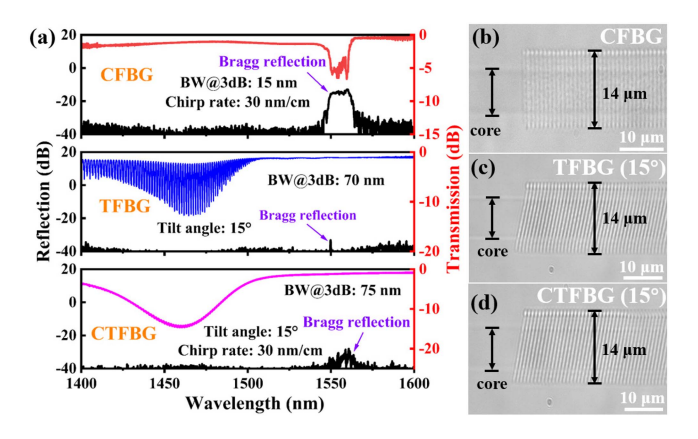


Fig. 2. (a) Transmission and reflection spectra and (b)–(d) top-view microscope images of the obtained CFBG ($\theta=0, \delta=30 \text{ nm/cm}$), TFBG ($\theta=15^{\circ}, \delta=0$) and CTFBG ($\theta=15^{\circ}, \delta=30 \text{ nm/cm}$) fabricated by using femtosecond laser LBL technology. BW@3dB: 3dB-bandwidth (based on the insertion loss level).

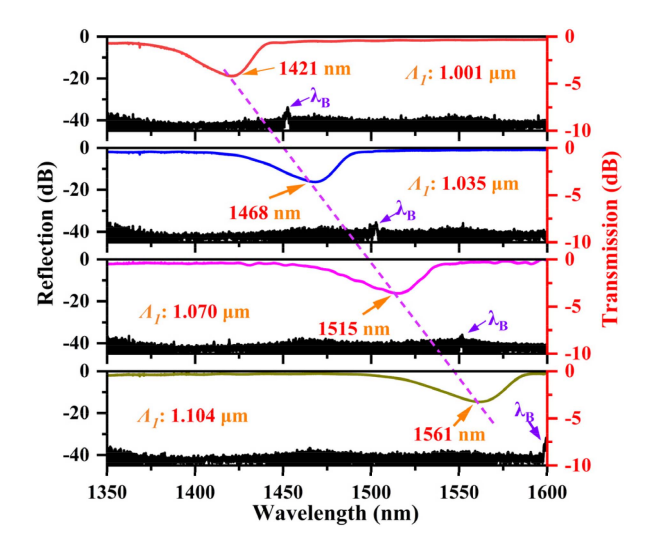


Fig. 3. Transmission and reflection spectra of the CTFBGs with different Λ_1 of 1.001 μm , 1.035 μm , 1.070 μm and 1.104 μm , respectively. $\lambda_B\colon Bragg$ wavelength.

Benefiting from the flexibility of femtosecond laser LBL technology, the spectra of CTFBGs with different initial pitch (Λ_1) were investigated. As shown in Fig. 3, when Λ_1 increased linearly from 1.001 μm to 1.035 μm , 1.070 μm and 1.104 μm , not only the Bragg wavelength of core mode increased linearly in long-wave direction (i.e., 1450 nm, 1500 nm, 1550 nm and 1600 nm), but also the central wavelength of the cladding mode coupling envelope (i.e., 1421 nm, 1468 nm, 1515 nm and 1561 nm), which meant that the central wavelength of such a filter could be easily and accurately customized via changing the initial pitch of the CTFBG. Here, except for Λ_1 , these CTFBGs were all fabricated with the same parameters, i.e., scanning velocity of 0.3 mm/s, pulse energy of 20 nJ, chirp rate δ of 30 nm/cm, tilt angle θ of 8°, and total length of 1 mm.

The tilt angle θ affects the phase matching condition of the grating as well as the coupling coefficient κ [6], thereby influencing the central wavelength and efficiency of the filter. As shown in Fig. 4(a), When the tilt angle θ was 4°, its 3 dB filtering

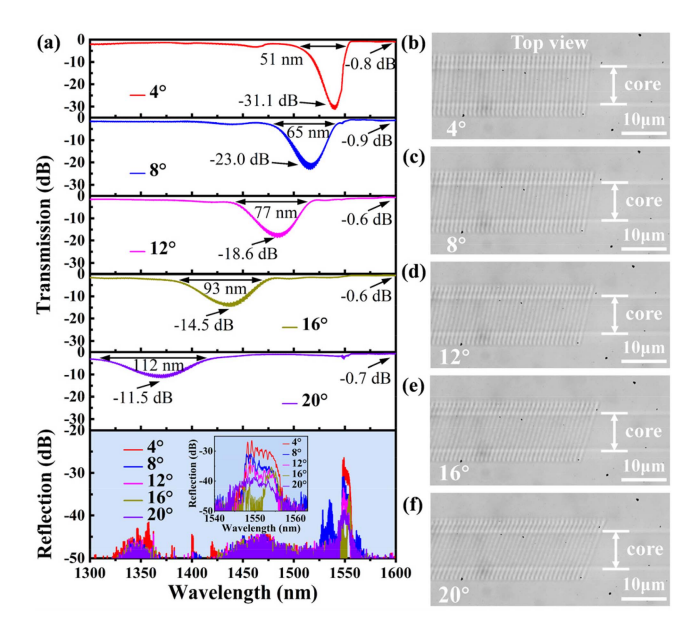


Fig. 4. (a) Transmission and reflection spectra and (b)–(f) top-view microscope images of the obtained CTFBGs with tilt angle θ of 4°, 8°, 12°, 16°, and 20°, respectively. The inset in (a) shows an enlarged view illustrating the decrease in Bragg reflection intensity with increasing tilt angle. Here, the bandwidths of the CTFBGs refer to the 3dB-bandwidths (based on the insertion loss level, the same below).

bandwidth could reach 51 nm, and the filtering efficiency could achieve a very high level of -31.1 dB (99.92%). As the θ gradually increased to 8°, 12°, 16°, and finally 20°, the 3 dB filtering bandwidth broadened to 65 nm, 77 nm, 93 nm, and 112 nm, respectively, while the filtering efficiency decreased to -23.0 dB (99.5%), -18.6 dB (98.6%), -14.5 dB (96.5%), and $-11.5 \, dB$ (92.9%), respectively. Therefore, by changing the tilt angle θ , a high-efficiency broadband-adjustable filter with a bandwidth ranging from 50 nm to over 110 nm and a filtering efficiency from >90% to >99.9% could be achieved. Note that the insertion loss of all CTFBGs was less than 1 dB. Additionally, as observed from the reflection spectra and the corresponding inset in Fig. 4(a), as the tilt angle θ increased, the Bragg reflection intensity of the CTFBGs gradually weakened from -30 dB to below -40 dB (close to the background noise), which could be beneficial for reducing its echo signal in applications such as communications. The reflection spectra exhibited a certain degree of non-flatness, which was caused by fabrication-induced modulation variations due to random stage jitter or local fiber microbending. As a result, this phenomenon is difficult to avoid. However, since the Bragg reflection is an unnecessary component, the non-flatness would not significantly affect the filtering performance of the CTFBG. Fig. 4(b)–(f) exhibit the top-view microscopic images of the CTFBGs with different tilt angles θ of 4°, 8°, 12°, 16°, and 20°, respectively. Here, the CTFBGs had the same chirp rate of 10 nm/cm, total length of 5 mm, and fabricating pulse energy of 20 nJ.

So far, by fixing the initial pitch Λ_1 and changing the tilt angle θ , the wavelength range of filtration could be flexibly selected. On this basis, by further changing the Λ_1 , the interval between the filtering wavelength and the Bragg reflection wavelength

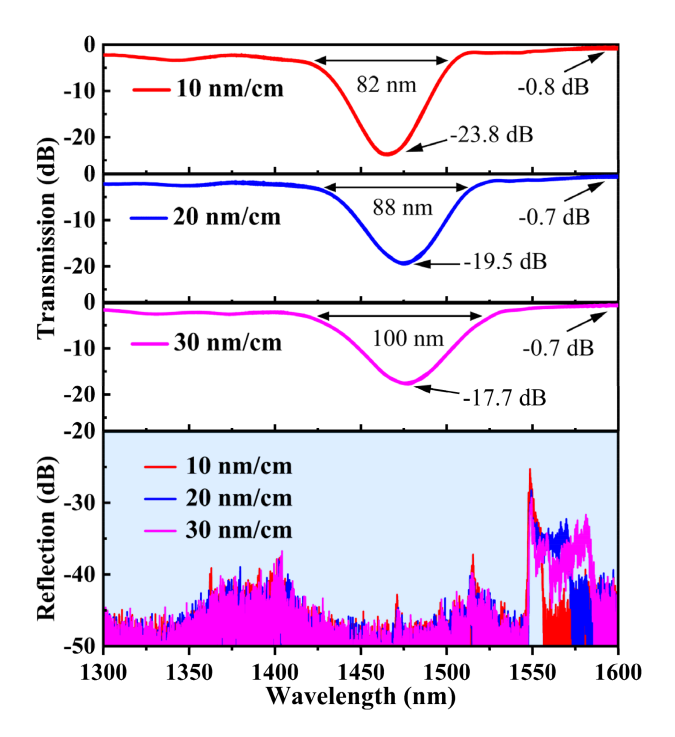


Fig. 5. Transmission and reflection spectra of the CTFBGs with different chirp rates of 10 nm/cm, 20 nm/cm and 30 nm/cm, respectively.

could be flexibly controlled. This enables a "filter & echo dual wavelength customization" to prevent extraneous Bragg reflection from affecting the transmission of normal light in the core.

Subsequently, to investigate the effects of different chirp rates on CTFBG's spectra, CTFBGs with different δ were also prepared. As shown in Fig. 5, as the chirp rate increased from 10 nm/cm to 20 nm/cm and then to 30 nm/cm, the filtering bandwidth of the CTFBGs expanded from 82 nm to 88 nm and 100 nm, respectively. This implies that by adjusting the chirp rate, the filtering bandwidth of CTFBG could be flexibly controlled. Meanwhile, the filtering efficiency of CTFBGs decreased from -23.8 dB (99.6%) to -19.5 dB (98.9%) and then to $-17.7 \, dB \, (98.3\%)$, respectively. This is because a larger chirp rate implies about fewer titled grating lines with close pitch, which will degenerate the strength of coupling between the forward-propagating core mode and each order backwardpropagating cladding modes. In addition, the central wavelength of the CTFBG exhibited a red shift, changing from 1465.8 nm to 1475.8 nm and then to 1477.4 nm. Moreover, from the reflection spectra shown in Fig. 5, it could be observed that as the chirp rate increased linearly, the Bragg reflection bandwidth also exhibited a linear increasing trend. Here, the initial pitch Λ_1 , tilt angle θ , and total length of the CTFBGs were 1.07 μ m, 12°, and 5 mm,

Furthermore, we have investigated the spectral characteristics of CTFBGs with different grating lengths. As shown in Fig. 6, when the length of the CTFBG was increased from 1 mm to 10 mm, the filtering depth improved from -5.4 dB (71.2%) to an exceptional -42.6 dB (99.995%). Meanwhile, the 3 dB bandwidth expanded from 35 nm to 104 nm. These results

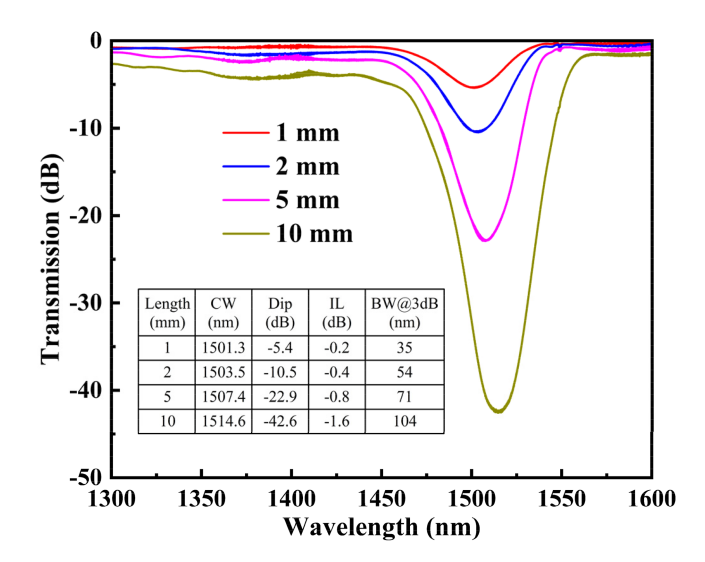


Fig. 6. Transmission spectra of the CTFBGs with different grating lengths of 1 mm, 2 mm, 5 mm and 10 mm, respectively. CW: Central wavelength; IL: insertion loss; BW@3dB: 3dB-bandwidth.

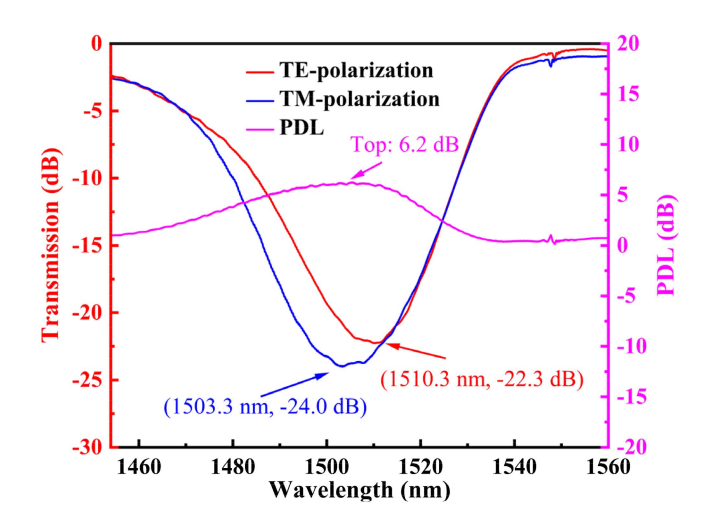


Fig. 7. Polarization dependence of CTFBG transmission spectrum. PDL: polarization dependent loss.

demonstrated that increasing the length could significantly enhance both the filtering efficiency and bandwidth of the CTFBG. In addition, a gradual increase in insertion loss was also observed with longer gratings. Moreover, the central wavelength exhibited a red shift from 1501.3 nm to 1514.6 nm. Here, the CTFBGs had the same tilt angle of 8° and a chirp rate of 10 nm/cm.

Subsequently, we have conducted polarization-dependent measurements of the CTFBG. In the experiment, a tunable laser source (N7776C, Keysight), an optical component analyzer (N7788C, Keysight), and an optical power meter (N7744A, Agilent Technologies) were used to characterize a CTFBG with a tilt angle of 8°, a length of 5 mm, and a chirp rate of 10 nm/cm. As shown in Fig. 7, when light with two orthogonal polarization states (TE and TM) was launched into the CTFBG, the transmission spectra exhibited certain distinctions. The central wavelengths of the cladding mode coupling envelopes were 1510.3 nm and 1503.3 nm for the TE and

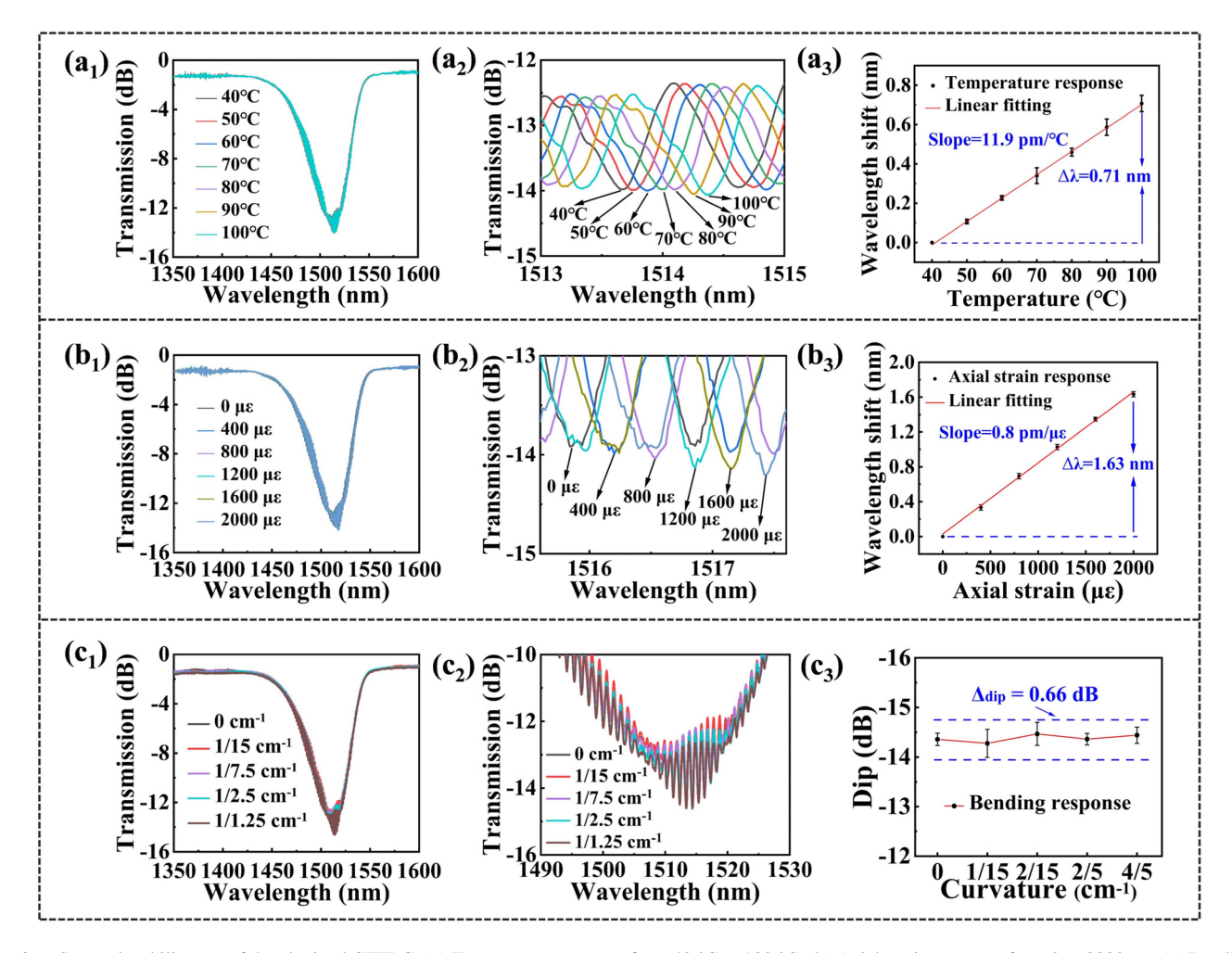


Fig. 8. Spectral stability test of the obtained CTFBG. (a) Temperature response from 40 °C to 100 °C. (b) Axial strain response from 0 to 2000 $\mu\varepsilon$. (c) Bending response: bending radius from infinity (no bending) to 1.25 cm, corresponding to the curvature from 0 to 4/5 cm⁻¹.

TM polarizations, respectively, and the corresponding filtering depths were –22.3 dB and –24.0 dB. This spectral discrepancy arose primarily because the modulation plane, which was tilted relative to the fiber axis, excited cladding modes with different polarization characteristics depending on the input polarization state [6]. Additionally, the measured polarization dependent loss (PDL) of the CTFBG reached a maximum value of 6.2 dB at a wavelength of 1505.3 nm.

The stability tests on the obtained CTFBGs, including temperature response, axial strain response and bending response, were also performed. The total length, tilt angle, and chirp rate of the tested CTFBG were 5 mm, 8°, and 30 nm/cm, respectively. Firstly, the temperature response was measured by placing the sample in a high-precision column oven (LCO 102) with an accuracy of 0.1 °C. The temperature range was set from 40 to 100 °C, with a holding time of 10 minutes at each measurement point, and three sets of measurements were conducted. Fig. 8(a1) illustrates the spectral changes for one set of measurement data, while Fig. 8(a2) provides a magnified view of the local spectra. As shown in Fig. 8(a3), the average wavelength shift and slope obtained from the three sets of measurements were 0.71 nm and 11.9 pm/°C, respectively. The error bars indicate that the

deviation at each measurement point was less than 0.1 nm. Next, the axial strain response of the CTFBG was measured by fixing one end of the CTFBG and stretching the other end attached to a translation stage. Three sets of measurements were performed, with the axial strain range from 0 to 2000 $\mu\varepsilon$. Fig. 8(b1)–(b2) present the spectral data and a magnified view of the local spectrum for one set of measurements. As shown in Fig. 8(b3), the average wavelength shift and slope derived from the three sets of measurements were 1.63 nm and 0.8 pm/ $\mu\varepsilon$, respectively. The deviation at each measurement point was also less than 0.1 nm. Finally, the bending response of the CTFBG was measured by placing it on a customized standard curvature plate. Measurements were taken at bending radii of ∞, 15 cm, 7.5 cm, 2.5 cm, and 1.25 cm (corresponding to curvatures of 0, 1/15 cm⁻¹, 1/7.5 cm⁻¹, 1/2.5 cm⁻¹, and 1/1.25 cm⁻¹, respectively), with three sets of measurements conducted for each condition. Fig. 8(c1)–(c2) display the spectral data and a magnified view of the local spectrum for one set of measurements. And as shown in Fig. 8(c3), the maximum dip variation of the CTFBG during the three measurements was 0.66 dB, with the deviation at each measurement point being less than 0.5 dB. Therefore, the experimental results demonstrate that the fabricated CTFBG

TABLE I				
COMPARISON OF TYPICAL PARAMETERS OF FIBER GRATING-BASED				
BAND-REJECTION FILTERS				

Reference	Device	Bandwidth (nm)	Efficiency	Length (mm)
[1], [26],[27]	FBG	0.1-10	Up to >99.99%	0.1-20
[3],[4], [28],[29]	CFBG	1-50	<90%	15-50
[5],[6], [30]	TFBG	20-100	Up to >99.9%	5-20
[7],[8], [31]	LPFG	20-200	Up to >99.9%	10-50
This work	CTFBG	51-112	Up to >99.99%	5

exhibits strong spectral stability and consistent filtering performance under a wide range of temperature, axial strain, and bending conditions. Combined with the maintaining of fiber coating, it could be deduced that the obtained CTFBGs have the ability to work stably under many complex environmental conditions.

Table I compares the typical parameters of existing fiber grating-based band-rejection filters. In terms of bandwidth, FBG-based and CFBG-based band-rejection filters are suitable for narrow-band (0.1 nm-10 nm) and moderate-band (1 nm-50 nm) filtering applications, respectively. In contrast, TFBG and LPFG are more appropriate for broadband filtering applications (>50 nm). Regarding filtering efficiency, CFBG typically has a relatively lower efficiency (<90%) due to the chirp effect. On the other hand, TFBG and LPFG exhibit significantly higher filtering efficiencies, up to >99.9%. Conventional FBG, primarily influenced by its length, can readily achieve an exceptionally high efficiency of >99.99%. Concerning device length, FBG and TFBG exhibit relatively short lengths, ranging from 0.1 mm to 20 mm and 5 mm to 20 mm, respectively. Due to inherent design constraints, CFBG and LPFG typically require longer lengths, ranging from 15 mm to 50 mm and 10 mm to 50 mm, respectively. Compared to these filters, the CTFBG fabricated in this work demonstrates an exceptional combination of large bandwidth (51 nm-112 nm), ultra-high efficiency (up to >99.99%), and a relatively short length (5 mm). Furthermore, compared to TFBG, the proposed CTFBG exhibits a smooth transmission spectrum, resulting in an optimized slope efficiency. Additionally, in contrast to LPFG, this CTFBG effectively minimizes environmental disturbances, thereby achieving enhanced filtering stability. Owing to the above-mentioned advantages, the proposed CTFBG has significant potential in high-quality broadband filtering applications.

IV. CONCLUSION

In conclusion, we have proposed and demonstrated a CTFBGbased band-rejection filter which is fabricated by femtosecond laser line-by-line technology. The experimental results show that CTFBGs combine the characteristics of wide bandwidth, high transmission loss, and smooth spectral envelope. The spectral characteristics, such as wavelength, bandwidth, and transmission loss, cloud be customized by CTFBG fabrication parameters (initial pitches, tilt angles, and chirp rates). By increasing the grating lengths of CTFBGs, large bandwidth and ultra-high filtering efficiency could be simultaneous realized at selected wavelengths. Furthermore, the spectral stability of the obtained CTFBG under the change of temperature, axial strain and bending have been verified. Flexible wavelength adjustment capability (filter & echo dual wavelength customization), coupled with low insertion loss (<1 dB), broadband-adjustable bandwidth (51 nm-112 nm), high filtering efficiency (up to >99.99%), negligible back-reflection (< -30 dB), and insensitivity to temperature, axial strain and bending, the proposed CTFBGs have the strong potential to be applied to high-quality fiber band-rejection filters, edge filters and gain equalizers applications.

REFERENCES

- J. Canning, D. C. Psaila, Z. Brodzeli, A. Higley, and M. Janos, "Characterization of apodized fiber Bragg gratings for rejection filter applications," *Appl. Opt.*, vol. 36, no. 36, pp. 9378–9382, Dec. 1997.
- [2] D. R. Chen, T. J. Yang, J. J. Wu, L. F. Shen, K. L. Liao, and S. L. He, "Band-rejection fiber filter and fiber sensor based on a Bragg fiber of transversal resonant structure," *Opt. Exp.*, vol. 16, no. 21, pp. 16489–16495, Oct. 2008.
- [3] X. Dong, P. Shum, X. Yang, M. F. Lim, and C. C. Chan, "Bandwidth-tunable filter and spacing-tunable comb filter with chirped-fiber Bragg gratings," Opt. Commun., vol. 259, no. 2, pp. 645–648, Feb. 2006.
- [4] Y. G. Han, X. Y. Dong, C. S. Kim, M. Y. Jeong, and J. H. Lee, "Flexible all fiber Fabry-Perot filters based on superimposed chirped fiber Bragg gratings with continuous FSR tunability and its application to a multiwavelength fiber laser," Opt. Exp., vol. 15, no. 6, pp. 2921–2926, Mar. 2007.
- [5] C. W. Haggans, H. Singh, W. F. Varner, Y. W. Li, and M. Zippin, "Narrow-band rejection filters with negligible backreflection using tilted photoinduced grating in single-mode fibers," *IEEE Photon. Technol. Lett.*, vol. 10, no. 5, pp. 690–692, May 1998.
- [6] J. Albert, L. Y. Shao, and C. Caucheteur, "Tilted fiber Bragg grating sensors," *Laser Photon. Rev.*, vol. 7, no. 1, pp. 83–108, Jan. 2013.
- [7] A. M. Vengsarkar, P. J. Lemaire, J. B. Judkins, V. Bhatia, T. Erdogan, and J. E. Sipe, "Long-period fiber grating as band-rejection filters," *J. Lightw. Technol.*, vol. 14, no. 1, pp. 58–65, Jan. 1996.
- [8] P. Wang, H. Zhao, T. Yamakawa, and H. Li, "Polarization-independent flat-top band-rejection filter based on the phase-modulated HLPG," *IEEE Photon. Technol. Lett.*, vol. 32, no. 3, pp. 170–173, Feb. 2020.
- [9] Y. Liu, L. Zhang, and I. Bennion, "Fabricating Fibre edge filters with arbitrary spectral response based on tilted chirped grating structures," *Meas. Sci. Technol.*, vol. 10, no. 1, pp. L1–L3, Jan. 1999.
- [10] F. Liu et al., "Wideband-adjustable reflection-suppressed rejection filters using chirped and tilted fiber gratings," *Opt. Exp.*, vol. 22, no. 20, pp. 24430–24438, Oct. 2014.
- [11] H. Li et al., "Robust femtosecond-written chirped and tilted fiber Bragg gratings for Raman filtering in multi-kW fiber lasers," Opt. Lett., vol. 48, no. 14, pp. 3697–3700, Jul. 2023.
- [12] M. Wang, Z. Li, L. Liu, Z. Wang, X. Gu, and X. Xu, "Fabrication of chirped and tilted fiber bragg gratings on large-mode-area doubled-cladding fibers by phase-mask technique," *Appl. Opt.*, vol. 57, no. 16, pp. 4376–4380, Jun. 2018
- [13] H. Song et al., "SRS suppression in multi-kW fiber lasers with a multiplexed CTFBG," Opt. Exp., vol. 29, no. 13, pp. 20535–20544, Jun. 2021.
- [14] P. J. Lemaire, R. M. Atkins, V. Mizrahi, and W. A. Reed, "High pressure H₂ loading as a technique for achieving ultrahigh UV photosensitivity and thermal sensitivity in GeO₂ doped optical fibres," *Electron. Lett.*, vol. 29, no. 13, pp. 1191–1193, Jun. 1993.
- [15] J. Canning, H. J. Deyerl, H. R. Sorensen, and M. Kristensen, "Ultravioletinduced birefringence in hydrogen-loaded optical fiber," *J. Appl. Phys.*, vol. 97, no. 5, Mar. 2005, Art. no. 053104.

- [16] S. J. Mihailov, D. Grobnic, C. W. Smelser, P. Lu, R. B. Walker, and H. Ding, "Chemical and physical changes induced in optical materials under highintensity laser irradiation," *Laser Chem.*, vol. 2008, 2008, Art. no. 416251.
- [17] J. Thomas, C. Voigtländer, R. G. Becker, D. Richter, A. Tünnermann, and S. Nolte, "Femtosecond pulse written fiber gratings: A new avenue to integrated fiber technology," *Laser Photon. Rev.*, vol. 6, no. 6, pp. 709–723, Nov. 2012.
- [18] J. He, B. Xu, X. Xu, C. Liao, and Y. Wang, "Review of femtosecond-laser-inscribed Fiber Bragg gratings: Fabrication technologies and sensing applications," *Photon. Sens.*, vol. 11, no. 2, pp. 203–226, Jun. 2021.
- [19] L. Chen et al., "High-quality fiber Bragg grating inscribed in ZBLAN fiber using femtosecond laser point-by-point technology," *Opt. Lett.*, vol. 47, no. 14, pp. 3435–3438, Jul. 2022.
- [20] K. Zhou, M. Dubov, C. Mou, L. Zhang, V. K. Mezentsev, and I. Bennion, "Line-by-line Fiber Bragg grating made by femtosecond laser," *IEEE Photon. Technol. Lett.*, vol. 22, no. 16, pp. 1190–1192, Aug. 2010.
- [21] A. Theodosiou et al., "Er/Yb double-clad Fiber laser with fs-laser inscribed plane-by-plane chirped FBG laser mirrors," *IEEE Photon. Technol. Lett.*, vol. 31, no. 5, pp. 409–412, Mar. 2019.
- [22] T. Duan, X. Li, R. Wang, F. Chen, and X. Qiao, "Femtosecond laser planeby-plane inscription of chirped and tilted fiber Bragg gratings," *J. Lightw. Technol.*, vol. 42, no. 17, pp. 6083–6089, Sep. 2024.
- [23] M. Wang et al., "Fabrication of chirped and tilted fiber Bragg gratings and suppression of stimulated Raman scattering in fiber amplifiers," *Opt. Exp.*, vol. 25, no. 2, pp. 1529–1534, Jan. 2017.
- [24] X. Tian, X. F. Zhao, M. Wang, and Z. F. Wang, "Effective suppression of stimulated Raman scattering in direct laser diode pumped 5 kilowatt fiber amplifier using chirped and tilted fiber Bragg gratings," *Laser Phys. Lett.*, vol. 17, no. 8, Aug. 2020, Art. no. 085104.
- [25] X. F. Zhao, X. Tian, M. Wang, H. Y. Li, B. Y. Rao, and Z. F. Wang, "Design and fabrication of wideband chirped tilted fiber Bragg gratings," Opt. Laser Technol., vol. 148, Apr. 2022, Art. no. 107790.
- [26] K. Guo et al., "High-spatial-resolution high-temperature sensor based on ultra-short fiber Bragg gratings with dual wavelength differential detection," J. Lightw. Technol., vol. 40, no. 7, pp. 2166–2172, Apr. 2022.
- [27] J. K. Sahota, N. Gupta, and D. Dhawan, "Fiber Bragg grating sensors for monitoring of physical parameters: A comprehensive review," *Opt. Eng.*, vol. 59, no. 6, Jun. 2020, Art. no. 060901.
- [28] D. Tosi, "Review of chirped Fiber Bragg grating (CFBG) Fiber-optic sensors and their applications," Sensors, vol. 18, no. 7, Jul. 2018, Art. no. 2147.
- [29] R. Min et al., "Largely tunable dispersion chirped polymer FBG," *Opt. Lett.*, vol. 43, no. 20, pp. 5106–5109, Oct. 2018.
- [30] T. Guo, F. Liu, B. O. Guan, and J. Albert, "Tilted fiber grating mechanical and biochemical sensors," *Opt. Laser Technol.*, vol. 78, part B, pp. 19–33, Apr. 2016.
- [31] F. Chiavaioli, F. Baldini, S. Tombelli, C. Trono, and A. Giannetti, "Biosensing with optical fiber gratings," *Nanophotonics*, vol. 6, no. 4, pp. 663–679, Jul. 2017.

Yu Fan was born in Guangdong, China, in 1999. He received the B.S. degree in 2021, from the College of Physics and Optoelectronic Engineering, Shenzhen University, Shenzhen, China, where he is currently working toward the Ph.D. degree. His current research interests include fiber Bragg gratings and high-power fiber lasers.

Weijia Bao received the B.S. degree in electronic information science and technology from Xidian University, Shaanxi, China, in 2013, and the Ph.D. degree in optics with Northwest University, Xi'an, China, in 2018. He is currently a Assistant Professor with the College of Physics and Optoelectronic Engineering, Shenzhen University, Shenzhen, China. His current research interests include fiber grating inscription, micromaching, and fiber sensing technology.

Cailing Fu received the M.S. degree in optical engineering from the Wuhan Institute of Technology, Wuhan, China, in 2015, and the Ph.D. degree in optical engineering from Shenzhen University, Shenzhen, China, in 2018. From 2018 to 2020, she was a Postdoctoral Research Fellow with Information and Communication Engineering, Shenzhen University, where she has been an Associate Professor, since 2020. Her current research focuses on distributed optical fiber sensing technology.

Changrui Liao received the B.Eng. degree in optical engineering and the M.S. degree in physical electronics from the Huazhong University of Science and Technology, Wuhan, China, in 2005 and 2007, respectively, and the Ph.D. degree in electrical engineering from Hong Kong Polytechnic University, Hong Kong, in 2012. Since 2013, he has been with Shenzhen University, Shenzhen, China, as an Assistant Professor/Associate Professor/Full Professor. His research interests include femtosecond laser micromachining, optical fiber sensors, and opto-microfluidics.

Yiping Wang was born in Chongqing, China, in 1971. He received the B.Eng. degree in precision instrument engineering from the Xi'an University of Technology, Xi'an, China, in 1995, and the M.S. and Ph.D. degrees in optical engineering from Chongqing University, Chongqing, China, in 2000 and 2003, respectively. From 2003 to 2005, he was with Shanghai Jiao Tong University, Shanghai, China, as a Postdoctoral Fellow. From 2005 to 2007, he was with The Hong Kong Polytechnic University, Hong Kong, as a Postdoctoral Fellow. From 2007 to 2009, he was with the Leibniz Institute of Photonic Technology, Jena, Germany, as a Humboldt Research Fellow. From 2009 to 2011, he was with the Optoelectronics Research Centre, University of Southampton, Southampton, U.K., as a Marie Curie Fellow. Since 2012, he has been with Shenzhen University, Shenzhen, China, as a Distinguished Professor. He has authored or coauthored one book, 21 patent applications, and more than 240 journal and conference papers. His current research interests include optical fiber sensors, fiber gratings, and photonic crystal fibers. He is currently a Senior Member of the Optical Society of America and the Chinese Optical Society.